Journal of Geodesy (2002) 76: 307–316
Doi 10.1007/s00190-002-0255-8

Journal of Geodesy

© Springer-Verlag 2002

Short-arc analysis of intersatellite tracking data in a gravity mapping mission

D. D. Rowlands[1], R. D. Ray[1], D. S. Chinn[2], F. G. Lemoine[1]

[1] Space Geodesy Branch, NASA Goddard Space Flight Center, Greenbelt, MD 20771, USA
e-mail: drowland@helmert.gsfc.nasa.gov; Tel.: +1-301-614-6110; Fax: +1-301-614-6099
[2] Raytheon ITSS, Code 926, NASA/GSFC, Greenbelt, MD 20771, USA

Received: 26 June 2001 / Accepted: 21 January 2002

Abstract. A technique for the analysis of low–low intersatellite range-rate data in a gravity mapping mission is explored. The technique is based on standard tracking data analysis for orbit determination but uses a spherical coordinate representation of the 12 epoch state parameters describing the baseline between the two satellites. This representation of the state parameters is exploited to allow the intersatellite range-rate analysis to benefit from information provided by other tracking data types without large simultaneous multiple-data-type solutions. The technique appears especially valuable for estimating gravity from short arcs (e.g. less than 15 minutes) of data. Gravity recovery simulations which use short arcs are compared with those using arcs a day in length. For a high-inclination orbit, the short-arc analysis recovers low-order gravity coefficients remarkably well, although higher-order terms, especially sectorial terms, are less accurate. Simulations suggest that either long or short arcs of the Gravity Recovery and Climate Experiment (GRACE) data are likely to improve parts of the geopotential spectrum by orders of magnitude.

Keywords: Geopotential determination – Satellite geodesy – Satellite-to-satellite tracking – GRACE

1 Introduction

For more than three decades the geodetic community has realized that satellite-to-satellite tracking (SST) provides extremely strong observational constraints for determining the geopotential (see e.g. Wolff 1969; Vonbun 1972). High–low satellite configurations have proven valuable in the past (see e.g. Kahn et al. 1982), and they continue to do so today (Lemoine et al. 1998b; Schwintzer et al. 2000). Low–low satellite configurations are expected to yield orders-of-magnitude improvements in geopotential definition (National Research Council 1997), and such a system may finally come to fruition in the near future with the Gravity Recovery and Climate Experiment (GRACE) mission (Tapley and Reigber 2000).

Methods for deducing the geopotential from low–low SST data have been developed by many groups over the past two decades (see e.g. Douglas et al. 1980; Kaula 1983; Wagner 1983, 1987; Colombo 1984; Jekeli and Upadhyay 1990). Many of these methods were based on semi-analytic theories that made various simplifying assumptions to overcome computational limitations. For example, both Kaula's and Colombo's methods assumed perfectly polar orbits – a 'tail-biting orbit' was Colombo's colorful phrase – which allow, among other advantages, fast Fourier techniques. Computational limitations are still an important consideration today, but not nearly so much as when these earlier works were written.

This paper explores a direct approach to estimating gravity from SST data, relying more heavily on numerical integration methods than on analytic or semi-analytic methods. We present extensive simulations with the following SST scenario: near-polar low–low satellites, separated by a couple of hundred kilometers, each satellite tracked continuously by global positioning system (GPS) and each deployed with accelerometers to correct for non-conservative forces. The fundamental measurement is the satellite-to-satellite range rate, measured with a precision of order 1 $\mu m\ s^{-1}$.

In addition to establishing a viable technique for the handling of SST data, this paper addresses two key questions for any practical data analysis.

1. To what extent is the SST gravity inversion insensitive to ephemeris accuracy? Specifically, is it sufficiently insensitive that the orbit determination and the gravity inversion can be performed in separate, independent steps?

Correspondence to: D. D. Rowlands

2. To what extent is the SST gravity inversion dependent on arc length? In particular, if the accelerometers are incapable of removing all non-conservative forces, including thrusting events, the satellite data might necessarily be broken into very short arcs. How will the gravity estimation be affected?

Concerning (1), our simulations described below show that, indeed, the SST data can be handled (within limitations) independently of the GPS data. We validate a two-step method. The first step concentrates only on achieving orbit accuracy (no gravity estimation). The second step uses only the SST data to refine certain components of the orbit while estimating gravity coefficients. (This method is somewhat analogous to what has been done to adjust tracking station coordinates from satellite laser ranging data; Sinclair and Appleby 1993.) A great advantage of this in our application is that the orbit determination task in an SST mission can concentrate on ephemeris accuracy, using techniques such as empirical accelerations that are normally prohibited in standard satellite gravity estimation. A second practical advantage is, of course, that the gravity inversion task can be performed without the considerable simultaneous data processing chores associated with GPS orbit determination.

The next section compares the role of arc length in conventional orbit-determination-based gravity estimation with the role it may play in a GRACE-like SST mission. Section 3 describes a transformation that we apply to the standard orbit parameters to enable our decoupled analysis of the SST data. Section 4 gives the rationale behind our data simulation procedures as well as a detailed description of those procedures. Sections 5 and 6 present results of parameter estimations using simulated data. Section 5 concentrates on the estimation strategy for orbit parameters, while Sect. 6 presents the results of gravity field recoveries with orbit parameters adjusting simultaneously.

2 Arc length in gravity estimation

When satellite tracking data are analyzed for geophysical parameter recovery, the analysis is often part of a simultaneous solution for orbit parameters. In such settings it is usually necessary to group the tracking data into 'arcs' of data which span multiple revolutions of the satellite. This is because most tracking data types do not provide enough geometric strength to provide a unique solution for the orbit until a substantial portion of the trajectory is examined. Furthermore, force model parameters like gravity coefficients build up sensitivity with arc length, because gravity signal is usually detected through its effect on the trajectory of a satellite. If two trajectories for a satellite are computed, each starting from the same initial conditions but using different gravity models, it usually takes some period of time from the initial epoch before differences in the trajectories are large enough that differences in the gravity signal can be inferred from tracking data. The trajectories are used to compute 'theoretical' values of the tracking data observations to which the actual observations are compared. The difference in the trajectories due to gravity needs to affect the computation of the theoretical tracking data values above the level of the precision of the actual tracking data. Furthermore, the differences in trajectories computed with different gravity models are often diminished because the initial state estimation process at some level accommodates gravity errors. Gravity is really an 'indirect effect' in conventional tracking data analysis. Arc length is required for the indirect effect to make its presence felt.

In general, long arcs are desirable. On the other hand, as the arc length grows, so does the effect of unmodeled forces. Therefore, the length of an arc in an orbit solution cannot be extended indefinitely without degrading the solution. Choice of arc length is a key decision in the analysis of tracking data. It depends on the geometric strength of the tracking data, the magnitude of unmodeled forces, and the sensitivity of the data to the geophysical parameters of interest. Gravity models like EGM96 (Lemoine et al. 1998a) have typically used tracking data analyzed in arcs of data from 1 to 30 days. With very few exceptions, the tracking data used in EGM96 would not support the extraction of gravity signal from an arc of data significantly shorter than a day.

In a gravity mapping mission where there is very precise tracking of the change in range between two satellites in the same orbit plane, many of the conditions that have always been a factor in deciding arc length for solutions using conventional tracking data will be very different. The most obvious difference is the high precision of the data. Small trajectory changes are detectable with more precise data. Furthermore, the intersatellite observation is, in some sense, a direct measurement of the difference in forces which the satellites experience at each instant, and hence almost a direct measurement of gravity (Colombo 1984). The extraction of gravity signal from such a measurement is unlikely to require the type of trajectory analysis that conventional tracking data requires. A precise range-change measurement between two satellites in the same orbit plane immediately senses the direct effect of gravity as well as the more latent indirect effect (effect on trajectory) that conventional tracking data rely upon exclusively.

The orbit determination aspects of a gravity mapping mission place different requirements on arc length as well. Precise range change measurements between two satellites do not provide sufficient information to determine independently the orbits of the two satellites. As will be demonstrated below, these measurements are extremely sensitive to some components of the orbits of the two satellites and almost completely insensitive to others (relative to how well they can be determined from other tracking data types). If the initial epoch state vectors of the two satellites are determined with other tracking data types, it should be possible to use the range-change measurements by themselves to refine only certain components of the orbits. This has the potential

to allow shorter arcs. Orbit refinement does not place the same constraints on arc length as orbit determination.

Even if the use of short arcs in a gravity mission is possible, the question remains if their use is desirable. As mentioned above, the effect of unmodeled forces places an upper limit on the length of arcs. In a mission which relies on high-precision tracking, the tolerance for unmodeled forces is especially low. Accelerometry can reduce the level of unmodeled forces, but it remains to be seen how well accelerometry will mix with very precise tracking data. In other words, even with accelerometry, the level of unmodeled or mismodeled surface forces may be high compared with the level of gravity signal that can be detected by precise intersatellite range-rate measurements. If so, this may be a limiting constraint on arc length. Also, small thrusting events may be inadequately sampled by accelerometers or there may be small data gaps or noise. These situations are most straightforwardly handled by analyzing short arcs that avoid periods of anomalous accelerations. Finally, it is possible that, for some applications, short arcs are desirable. For example, short arcs may facilitate the independent analysis of regional data in the form of gravity anomaly blocks or some other local gravity parameterization. It is beyond the scope of this investigation to answer many of the questions surrounding the desirability of short-arc analysis. We intend to demonstrate the possibility of short-arc (under 15 minutes in length) analysis. We also explore the tradeoff between using short arcs and arcs of more conventional length (1 day), assuming that the longer arcs are possible within the constraints presented by a real gravity mapping mission.

3 A baseline representation for initial epoch state parameters

Orbit solutions often solve for the six Cartesian components of a satellite's state vector at an initial epoch. After each iteration of an orbit solution, the updated initial Cartesian state vector is used to compute the trajectory at later epochs, which is accomplished by numerical integration of the Cartesian components of the state vector. Even though the initial epoch state vector is required in Cartesian form, it is sometimes useful to solve for an alternative representation of the initial state vector – for example, osculating Kepler elements. Often it is easier to apply useful constraint equations that are applicable to a particular data type when a non-Cartesian representation is used. After the alternative form of the state vector is updated, it is transformed to Cartesian coordinates and the numerical integration proceeds. It is straightforward to convert an orbit solution from a Cartesian state vector solution to some other representation. All that is required is the six-by-six matrix of the partial derivatives of the six initial Cartesian state vector parameters with respect to the six alternative parameters.

In the case of the two satellites of a gravity SST mission, the 12 parameters describing the two initial Cartesian state vectors can be converted to the Cartesian state vector of the baseline (the difference vector) between the two satellites and the Cartesian state vector of the baseline midpoint (the average of the two satellite state vectors). These two vectors can be further transformed. In the case of the midpoint state vector, it is useful to convert the three position components to spherical coordinates: the declination of the midpoint, the right ascension of the midpoint, and the distance between the midpoint and the Earth's center of mass. For the baseline vector, it is useful to imagine a local Cartesian coordinate system centered at the midpoint of the baseline. The XY plane of the system is perpendicular to the position vector of the system midpoint. The X axis is the local east vector of the local coordinate system. It is further useful to describe both the position and velocity (rate of change) components of the baseline state vector in spherical coordinates which are based in this local coordinate system. In each case, the vector is converted to magnitude, pitch (angle the vector makes with XY plane) and yaw (angle that the projection onto the XY plane makes with the X axis). The 12 new epoch state parameters are:

- P_1 distance of baseline midpoint from the Earth's center of mass
- P_2 declination of baseline midpoint
- P_3 right ascension of baseline midpoint
- P_4 inertial X component of baseline midpoint velocity vector
- P_5 inertial Y component of baseline midpoint velocity vector
- P_6 inertial Z component of baseline midpoint velocity vector
- P_7 baseline vector length
- P_8 baseline vector pitch
- P_9 baseline vector yaw
- P_{10} baseline rate-of-change vector magnitude
- P_{11} baseline rate-of-change vector pitch
- P_{12} baseline rate-of-change vector yaw.

We have implemented the ability to solve for the above 12 parameters in our orbit determination and geodetic parameter estimation software, GEODYN (Pavlis et al. 2001). This required only a new subroutine which transforms back and forth between a pair of Cartesian state vectors and the above 12 parameters and which also computes the 12 by 12 matrix of the partial derivatives of the 12 initial Cartesian state parameters with respect to the 12 spherical coordinate parameters.

In the following sections we demonstrate that the above 12 parameters are promising for use in the analysis of the intersatellite range-change measurements when they are decoupled from other tracking data types that might be available. We can reasonably expect that the intersatellite range-change measurement is more sensitive to the baseline parameters than to the midpoint parameters. We also expect that the intersatellite range-change measurement is fairly insensitive to the baseline yaw parameters. If the range-change measurements are to be analyzed independently from other tracking data

types (in the second step of our two-step method), then it is important to study the sensitivity of the range-change measurement to each of the above 12 parameters. The sensitivity of the measurement to each of the 12 parameters should be compared with how well each parameter is likely to be determined independently from other tracking data types available in the mission (in the first step of our two-step method). That subject is explored in Sect. 5 and in the Appendix.

Table 1. Initial Keplerian elements for both satellites[a]

Semi-major axis a	6 878 050 m
Eccentricity e	0.001
Inclination i	89.1°
Node Ω	0°
Perigee argument ϖ	0°
Mean anomaly m	0°
Period T	94.6 min

[a] Initial epoch satellite 2 = initial epoch satellite 1 + 30 s

4 Data simulation and assumptions for data reduction

This section is devoted to an explanation of the techniques and assumptions involved in simulating the data used in our study. Although the analysis of the data is explained in Sects. 5 and 6, it is useful to lay out the goals of the data analysis before proceeding with a description of the data simulation. The analysis is intended to reveal the extent to which gravity recovery can be achieved from short-arc solutions. This we intend to do in a relative sense by comparing the results obtained from short arcs to the results obtained from arcs of more traditional length. Of course, the results in each case use simulated data and are likely to be optimistic. It is the differences in results which are most instructive. We perform the short-arc analysis and long-arc analysis under nearly identical circumstances. While the 'burden of proof' falls upon the less traditional short-arc analysis, we have tried to ensure that simplifying assumptions used in the data simulation procedure will have equal effect on both analyses. In any case, we do not want an assumption to favor the short-arc analysis.

Accelerometry is one example where simplifying assumptions were made. For the long-arc analysis we assumed that there are no problem epochs associated with the accelerometry (gaps or inadequately sampled thrusts). As will be described further below, in the short-arc analysis we assumed that problem epochs occur fairly frequently. Obviously, this favors the long-arc analysis. We also assumed that the accelerometry is error free (other than at problem epochs for short arcs). Although this assumption makes both analyses optimistic, it favors the long-arc analysis. In practice, short arcs are less affected by accelerometry errors because there is less time for the errors to grow as they are integrated in the satellite force model. Problems associated with errors in surface forces (whether they come from surface force models or from accelerometry) have traditionally been a limiting constraint on arc length. An error-free accelerometry assumption favors the long-arc solution.

All of the studies in this paper are based on using simulated one-way intersatellite range-rate data with a Doppler counting interval of 1 s. The data were generated using the orbits of two co-orbiting satellites with characteristics shown in Table 1. The key points are that the satellites are at an altitude very close to 500 km, have a very low eccentricity, are very nearly polar, and are separated by about 200 km. The second satellite's initial elements are an exact copy of the first satellite's initial elements 30 seconds later. This was done only as a matter of convenience in the data simulation step, and was no way exploited in the data analysis step. Furthermore, the orbits of the two satellites evolve a bit differently, because (as described below) thrusting events were assigned to each satellite at different epoches in the simulation step.

The satellite orbits were generated with the EGM96 gravity field using all terms up to degree 120. Drag and solar radiation were not modeled in our simulations; it is assumed that accelerometry will sufficiently account for these forces. Accelerometry should also compensate for small thrusting events, but it is possible that thrusting can cause occasional problems, so our simulations do include thrusting. Each satellite was given a thrust every 30 minutes (a ΔV of about 0.5 mm s^{-1}), but in a staggered manner so that the satellite–satellite system received a ΔV every 15 minutes. [This, in fact, is roughly comparable to the thrusting frequency currently occurring on the CHAMP satellite (Schwintzer et al. 2000).] Although it would be hoped that an accelerometer would accurately model thrusts, we wish to determine if problematic thrusts can be removed from the analysis process altogether (assuming they occur no more frequently than every 15 minutes). We therefore investigate whether gravity signal can be recovered while analyzing range-rate data in arcs of slightly less than 15 minutes (between thrusts). Orbits are refined every 15 minutes using arcs that begin 40 s after a thrust and 20 s before a thrust (14-minute arcs).

A data point was created every 5 s for 30 days (the counting interval remaining at 1 s). Two versions of the data were created, one with no noise and the other with noise of 1 μm s^{-1}. The noiseless version was useful in the verification of the modifications made to the GEODYN software for the new epoch state parameterization. The noiseless version was also used in preliminary studies to determine range-rate data sensitivity to epoch state parameters in orbit refinement solutions. The lack of noise makes residual analysis easier. All gravity recovery simulations used the data with noise.

Most of the studies in this paper involve reducing the simulated data using an a priori gravity field which is different from EGM96. A crucial question is to determine whether the intersatellite range-rate data can be used by themselves (after orbits have been precomputed with a variety of tracking types and then refined in certain components with the intersatellite measurements) to recover the coefficients of EGM96, starting from a different gravity field. The a priori gravity field is a 'clone' of

EGM96 through degree 70 and is zero above that. (By clone field, we mean a field that differs from the original by about the amount the original field differs from reality. Clones are often used in sensitivity studies like ours.) At degree 70 and below, the coefficients of the a priori clone field differ from EGM96 by about the standard errors of EGM96. While considerable evidence suggests that the EGM96 errors are realistic (Lemoine et al. 1998a), the EGM96 model itself does differ from some other recent models by amounts exceeding these errors. Our a priori clone gravity model should therefore be considered as fairly 'close' to EGM96, so if we are able to recover a field that is closer to EGM96 than the clone, then we will have shown that our technique is useful for recovery of small gravity signal below degree 70. Basing the test on an a priori field that is already close to EGM96 is a stringent test of sensitivity. Above degree 70, our test will be less severe since we are starting from zero (which is farther away from EGM96 than the standard errors). Even so, we will be able to determine if signal above degree 70 can be recovered with our method of reduction.

The clone field was also used to generate the starting trajectory that is used to obtain the a priori elements to begin the orbit refinement process (the second step of our two-step process, which also includes gravity estimation). The intersatellite range-rate data are used in this refinement step to adjust only three or four of the 12 initial state parameters (as discussed below). In the second step we accept the other eight or nine initial elements from the starting trajectory without alteration. So, some information from the starting trajectory (including errors) will be present in the final orbits that are used to extract the gravity signal. In the next section it will be shown that the intersatellite measurement is sensitive to some orbit components and insensitive to others. It is important that our study uses a starting trajectory that has been produced in a realistic manner so that it contains a realistic distribution of errors across all the orbit components.

Starting trajectories will almost certainly be produced with reduced dynamic techniques (see e.g. Bertiger et al. 1994; Rowlands et al. 1997). This involves the exploitation of dense tracking and aggressive empirical parameterizations to compensate for the fact that the gravity model and other aspects of the force model have errors. The empirical parameters are usually used in the form of acceleration coefficients that are valid over a specified period of time. Typically, empirical acceleration coefficients are used in the along- and cross-track directions. Every time the force model is evaluated during the time period of its validity, these extra accelerations are applied in the specified direction(s). Colombo (1989) demonstrates that empirical acceleration parameters are especially useful when of the form

$$A\cos(\omega + M) + B\sin(\omega + M)$$

where ω is the argument of perigee and M is the mean anomaly. The sum of these angles cycles through 360° each revolution, hence the name 'once-per-rev' empirical acceleration.

The solution for the starting trajectories had the following characteristics.

1. The clone gravity field was used.
2. ΔVs were solved for at the appropriate times.
3. Empirical, periodic once-per-revolution accelerations (A and B parameters) were solved for in both the along- and cross-track components. These parameters were estimated every 30 minutes.
4. The simulated intersatellite range-rate measurements were used as a tracking data type.
5. To simulate the strong geometrical constraints that GPS tracking would provide, the 'truth' ephemeris was used as a tracking data type in the position components only (velocity information not used).
6. Solutions used 30 h of data, from 0000 hours of one day to 0600 hours of the next.

The starting ephemeris produced from the above solution differs from the 'truth position' in a root-mean-square (RMS) sense by 3 cm (total position). That is probably optimistic for what will be attainable for the position components of a pair of satellites at 500 km altitude. This level of position accuracy was achieved in part because the position components of the truth ephemeris were used as a data type as a convenient substitute for GPS data. As Jekeli (1999) makes clear, the velocity components of the orbit are probably more important for our study. The above solution did not use the velocity components of the truth trajectory as a data type. The velocity components of our solution are evidently resolved on the strength of the intersatellite range-rate data. Those data were given a realistic treatment. The orbit solution for our starting ephemeris fits the intersatellite data at 12 μm s^{-1} (12 times the noise level) over a 30-h arc.

When judging whether our starting ephemeris is realistic, it is tempting to compare our results to the orbit solution performance currently being achieved for the CHAMP satellite (Reigber et al. 2000), which currently is roughly 10 cm. CHAMP is also in a polar orbit, but it is about 60 km lower than the satellites in our simulation. More importantly, CHAMP does not benefit from a precise intersatellite range-rate measurement. The intersatellite range-rate measurement contributes to the resolution of the many empirical acceleration parameters used in our reduced dynamic approach. A gravity mapping mission with a precise intersatellite range-rate measurement would have better orbit solution performance than a single satellite mission like CHAMP. In any case, in the Appendix we demonstrate that the use of a somewhat degraded version of our starting ephemeris has very little effect on gravity recovery.

5 Orbit refinement

Before attempting any large simulations to demonstrate the ability of our technique to recover gravity information, we performed some smaller simulations with the

goal of understanding orbit refinement from intersatellite measurements. In particular, we wished to determine which parameters need be refined and which parameters can be taken from the reduced dynamic trajectory without alteration.

Our first set of tests used the truth force model (EGM96 up to degree 120) and the noiseless intersatellite range-rate data. These tests were performed on short arcs (14 minutes) between the ΔV thrusting events described in the previous section. The goal of these tests was to find the best minimum set of initial state parameters to estimate so that the a posteriori range-rate residuals are well below the 1 μm s^{-1} level. If all of the elements are set to truth values, then the noiseless data fit perfectly when EGM96 is used. The unrefined initial elements are only close to the truth values and produce residuals of 200 μm s^{-1} even if the EGM96 gravity model is used. Although the data used in these tests were noiseless, they were weighted in the least-squares (LS) solution as if they had a standard deviation of 1 μm per second. This is noted so that the formal standard deviations of the adjusted parameters can be interpreted.

The first runs adjusted a single parameter. As noted above, the starting elements without refinement produce residuals with an RMS of about 200 μm s^{-1}. When only a single parameter is adjusted, the only parameter that could reduce the RMS residual to under 100 μm s^{-1} is the baseline rate-of-change pitch parameter P_{11}. In fact, the P_{11} adjustment produced an RMS residual of under 10 μm s^{-1}.

The second set of runs adjusted two parameters, with P_{11} always being one of the pair. While examining the choice of a second parameter it became clear that, over short arcs, two parameters are highly correlated: P_{10} (baseline rate-of-change magnitude) and P_1 (the distance of the baseline midpoint from the center of mass of the earth). The choice of either of these parameters as the second parameter to accompany P_{11} produces almost identical residual patterns. When these two parameters (P_{10} and P_1) are allowed to adjust simultaneously along with P_{11}, the inverted normal matrix shows a correlation between P_1 and P_{10} of very nearly one. When either of these two parameters accompanies P_{11}, the solution produces an RMS residual of less than 1 μm s^{-1}. We chose to use rate-of-change magnitude (P_{10}) because the adjustments in this component were always less than 100 μm s^{-1} and usually less than 20 μm s^{-1}. This seems more reasonable than the adjustments in the P_1 parameter (sometimes more than 30 cm), since our reduced dynamic trajectories were better than 10 cm radially. In general the P_1 parameter should almost always be determined from a reduced dynamic trajectory to better than 10 cm, so over short arcs this parameter is not likely to need adjustment.

Even though the adjustment of P_{10} and P_{11} brings the RMS residuals to under a 1 μm per second, there were noticeable trends in the residuals, sometimes near the micron-per-second level. Because of this we made one more set of runs to search for a third parameter. We find that baseline pitch P_8 works best. With P_8, P_{10}, and P_{11} adjusting, the RMS residuals were well under 0.1 μm s^{-1}. Therefore, in our short-arc gravity recovery experiments (next section) we adjusted these three parameters. It may be possible to avoid adjusting baseline pitch, especially if arcs of 10 minutes or less are attempted.

Our final set of runs deal with longer arcs. In the next section we describe two gravity field determinations. One determination uses 30 days of 14-minute arcs (2878 arcs). The other uses 30 arcs, each 1 day in length. We want to find the proper set of adjusting parameters for 1-day arcs. In extending to 2-h arcs we found that our '14 minute parameterization' (P_8, P_{10}, P_{11} adjusting) holds up quite well, producing fits of less than 0.2 μm s^{-1}. We also found that for arc lengths of 2 h, the P_1 parameter is still highly correlated with P_{10}. At an arc length of 12 h the '14-minute parameterization' produces RMS residuals of close to 1 μm s^{-1}. Also, at this arc length, the P_1 parameter is less correlated (still 0.999) with P_{10}. At 12 h and above, four parameters (including P_1) can be sensibly adjusted. In these adjustments the formal standard deviation of P_1 is less than 1 cm. When P_1 is adjusted as the fourth parameter in a 12-h arc, the RMS residual is reduced to below 0.1 μm s^{-1}. In a 24-h arc, the correlation between P_1 and P_{10} is reduced to 0.995. Our 'long arc' gravity analysis described in the next section simultaneously adjusts four arc parameters along with gravity coefficients.

As noted above, the noiseless version of the data was used in these orbit refinement studies and the force model was set to 'truth' values. So, if enough initial state parameters are allowed to adjust, the data will be fitted perfectly. The gravity analysis described in the next section uses the initial state parameterizations that have just been described, but the clone gravity field is used to compute the trajectories (refine the trajectories before normal equations are generated) and the 'noise-added' version of the data is used. In this mode, when the three short-arc parameters are allowed to adjust, the arcs fit the data between 7 and 25 μm s^{-1}. The day-long arcs, with four parameters adjusting, have fits between 20 and 60 μm s^{-1}.

6 Gravity solutions

The gravity solutions presented in this section are, like most simulations, somewhat optimistic. The simulations include no unmodeled effects other than random measurement noise and some initial satellite state error (which is left over from those initial satellite state elements that we leave unaltered from the reduced dynamic trajectory). In the long-arc analysis we modeled (without adjustment) the 'truth' values of the ΔV thrust events, which implies perfectly performing accelerometers. Futhermore, in addition to some initial satellite state refinement, only gravity parameters are estimated from the simulated data; no attempt is made to estimate, for example, tidal and gravity parameters simultaneously. In fact, tides and other high-frequency atmospheric and oceanic mass motions pose serious aliasing problems for an SST mission because of the difficulty in

modeling and removing the associated gravity effects at required accuracies (Zlotnicki et al. 2000; Verhagen et al. 2000). Such problems are here ignored.

The two solutions presented below, one comprising short arcs and the other comprising long arcs, are intended to be taken qualitatively. The differences between the short-arc solution and the long-arc solution are of particular interest, since they reveal how much information is potentially lost when short arcs are used and what can be gained by extending arc length (assuming the level of unmodeled forces does not preclude the use of long arcs). However, the fact that it is possible to obtain sensible gravity solutions from arcs shorter than 15 minutes is significant in itself.

We estimated two gravity fields using the 30 days of simulated data described in Sect. 4. Each gravity field was estimated to degree 120 without any constraints. The method used in estimating the fields differed in the choice of arc length. The 'short-arc' field used 2878 arcs 14 minutes in length, while the 'long-arc' field consisted of 30 arcs, each 1 day in length. The short-arc field estimated $2878 \times 3 = 8634$ arc (orbit) parameters simultaneously with the 14 337 gravity coefficients, while the long-arc field estimated $30 \times 4 = 120$ arc parameters. The short-arc field discarded 1 minute of data around each ΔV (12 points) every 15 minutes, so the short-arc field uses approximately 7% fewer observations.

The estimated gravity fields should be compared with EGM96, which was used to simulate the data and is therefore the 'true' field, and the EGM96 clone, which was used as the a priori field from which gravity normal equations and initial ephemerides were produced. The figures in this section which pertain to coefficient values show differences from EGM96. If our estimates were perfect, the estimated coefficient differences from EGM96 would be zero. Of course the differences are not zero, but they are much smaller than the differences between EGM96 and the EGM96 clone (see Fig. 2).

The formal errors of our estimated coefficients cannot be directly compared to EGM96 errors. The standard errors of EGM96 are the result of a complex calibration of weights of the many data types used in its solution (Lerch 1991). The formal errors of our two estimated fields are simply the diagonals of an inverted normal matrix having a single data type which had been assigned a standard deviation of 1 $\mu m\,s^{-1}$. The formal errors of our estimated gravity coefficients should therefore be interpreted only in a relative sense. Internally, they should be reliable for seeing which portions of the estimated gravity fields are more strongly or weakly determined. Externally, they should provide a good basis to compare two gravity fields that were estimated in a largely similar fashion.

Figure 1 shows the RMS differences of the prior field and the two estimated fields with respect to the 'true' EGM96. It shows immediately (and reassuringly) that both estimated fields are considerable improvements over the a priori field. Neither field appears to be impacted by the truncation of the prior field at degree 70; both show relatively smooth differences with respect to EGM96 through all degrees. More interestingly, Fig. 1

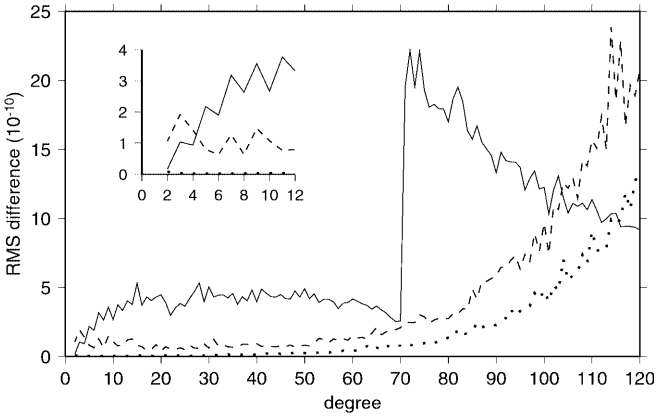

Fig. 1. RMS gravity coefficient differences with respect to a 'true' gravity field of the a priori field (*solid line*), a solution employing short arcs (*dashed line*), and a solution employing long arcs (*dotted line*). The discontinuity in the a priori model arises because it is truncated to zero above degree 70. The insert is a zoom view of the low degrees

emphasizes that an accurate gravity field can be estimated from short arcs. The short-arc gravity field is significantly better than the a priori field at every degree from degree 5 up to degree 100. It is not surprising that a field that is sewn together only from sub-orbital arcs is weaker at the very lowest degrees. The comparison of the performance (by degree) of the short-arc field with that of the long-arc field is not unfavorable to the short-arc field from degree 30 upwards. However, at about degree 100, the short-arc field stops out performing the clone gravity field. This does not happen until about degree 110 for the long-arc field. When judging the relative performance of the two estimated fields, it should be remembered that our simulations assume that the accelerometer is working perfectly (no unmodeled forces), which is much more beneficial to the outcome of the long-arc field than the short-arc field.

More detailed comparisons of the three fields are shown in Fig. 2, while the estimated formal errors are shown in Fig. 3. Over a wide range of degrees and orders, both estimated fields show remarkable improvements relative to the EGM96 clone. Many coefficients are improved by two orders of magnitude. This is generally consistent with figures quoted in the 1997 National Research Council report (see National Research Council 1997, Fig. 2.6), but it is more definitive since the National Research Council calculations were based on an analytic theory of Jekeli and Rapp (1980) which assumes isotropic data (including data at all inclinations) and ignores possible required arc parameters.

In general, Figs. 2 and 3 agree well and show where the solutions are strong and where they are weakened when arcs are shortened. For a given degree, both the short-arc and long-arc fields determine lower-order coefficients more accurately than higher-order coefficients. That trend is much more pronounced in the short-arc field, especially for sectorials, which for some low degrees are actually slightly inferior to the clone field. Again, this is not surprising – we cannot expect an extremely short arc (roughly 1/6 of a revolution) in a

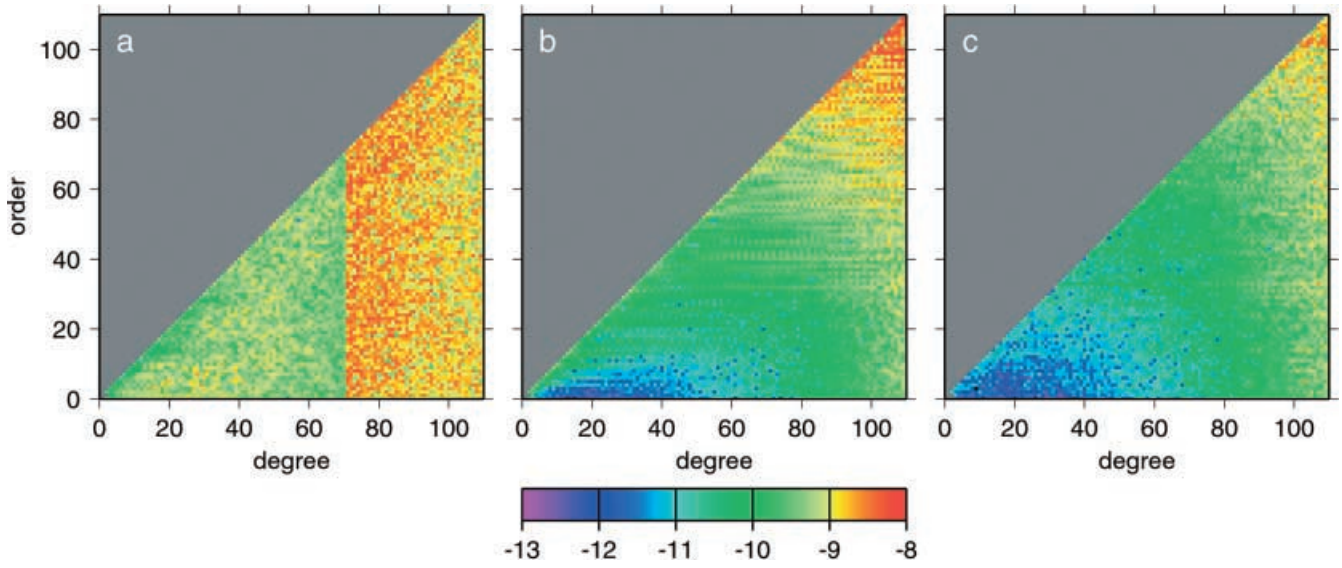

Fig. 2. Results of gravity inversion simulations showing $\log\sqrt{(\Delta C_{nm}^2 + \Delta S_{nm}^2)}$, for fully normalized Stokes coefficients C_{nm}, S_{nm} differenced with the 'true' gravity field, for **a** the a priori gravity field, **b** the short-arc gravity inversion, and **c** the long-arc gravity inversion. The discontinuity in the a priori model arises because it is truncated to zero above degree 70. Below degree 70 **a** is indicative of present-day uncertainties in the geopotential, as represented by the standard errors of EGM96

high-inclination orbit to be sensitive to long-wavelength sectorial terms.

Most remarkably, the long-arc and short-arc fields are very comparable at low orders, especially so for zonal coefficients. The RMS discrepancy over all degrees (2 to 120) between EGM96 and the short-arc field for zonal coefficients is 1.9×10^{-10}. For the long-arc field that discrepancy is 1.8×10^{-10}. Figure 4 shows that this striking similarity holds for all zonal terms, save the few between degrees 2 and about 8. For degrees 10 to 40 both long-arc and short-arc zonals are two orders of magnitude (or more) more accurate than the clone model. They are nearly one order of magnitude more accurate at degrees 40 to about 100. The improvement ceases at degree 112. Determining zonal gravity coefficients has historically been problematic in satellite geodesy. Clearly, an SST mission – even one which for one reason or another is restricted to using very short arcs of data – is likely to yield significant advances.

7 Summary

We have demonstrated a promising technique for the analysis of low–low intersatellite range-rate data from a gravity mapping mission. The technique largely (but not

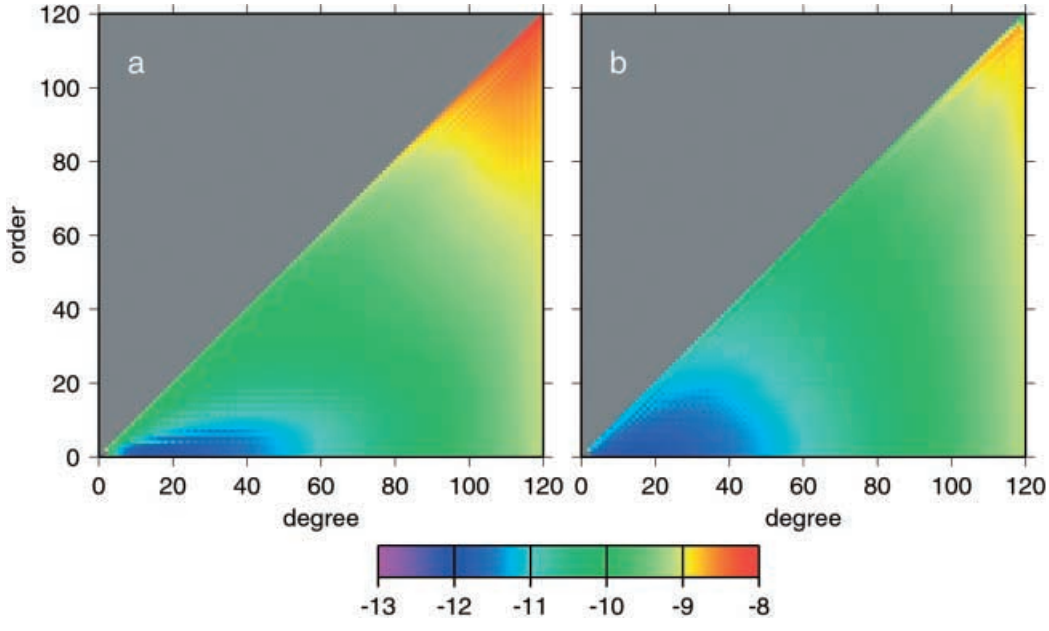

Fig. 3. Formal errors for gravity simulations employing **a** short arcs and **b** long arcs. Colors show the logarithm of errors for fully normalized coefficients

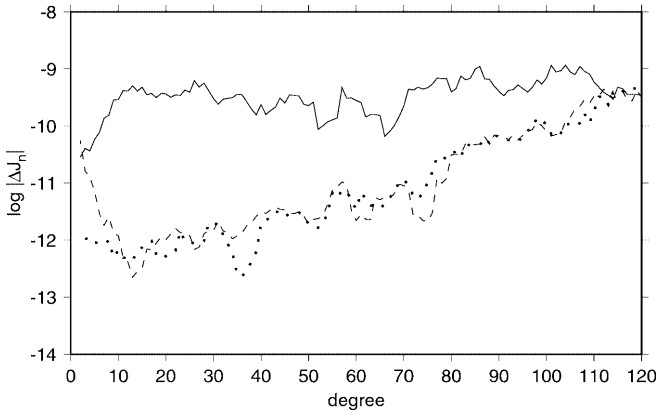

Fig. 4. Differences with respect to a 'true' gravity field of zonal coefficients J_n of degree n, for the a priori field (*solid line*), the short-arc gravity solution (*dashed line*), and the long-arc gravity solution (*dotted line*). All three lines have been smoothed to remove minor statistical variability (which smears out discontinuity in solid line at degree 70). The long-arc and short-arc solutions are similar, except for the lowest degrees where the short-arc solution is less accurate

completely) decouples the task of orbit determination from the task of extracting gravity information. This has several advantages.

1. In the first step of the procedure orbits can be determined using all available tracking types and reduced dynamic techniques. Extraction of gravity information in the second step benefits from the use of empirical accelerations used in the first step without aliasing problems.
2. In the second step of the procedure, only intersatellite data are used. Gravity information can be extracted without complex solutions involving multiple data types.
3. Because orbits are only refined (not fully determined) in the second step, short-arc analysis is facilitated.

The technique transforms the standard 12 initial epoch state vector parameters of the two satellites into spherical coordinates describing the baseline between the two satellites. We have performed an analysis to show which of these 12 parameters need to be estimated simultaneously with gravity coefficients.

We have used this technique to estimate gravity fields from simulated data. Our study neglects many effects, but unlike some simulation studies of gravity missions in the literature, we consider the need to estimate orbit parameters simultaneously with gravity coefficients. We have investigated the possibility of estimating a gravity field entirely from short arcs (14 minutes) of intersatellite range rate data and found that this should indeed be possible. We have also shown the differences between a short-arc gravity field and a field estimated from long arcs. The use of long arcs (if possible) adds information primarily at the higher orders of every degree of the gravity field.

Acknowledgements. The authors thank their colleagues S. Klosko and S. Luthcke for general discussions on satellite–satellite tracking and for specific discussions on this paper. C. Reigber, C. Jekeli, T. Otsubo, and G. Balmino are thanked for comments on the original manuscript. Computational facilities were provided by the NASA Center for Computational Sciences at Goddard Space Flight Center.

Appendix

In Sect. 5 we discussed an orbit refinement stratgey which (depending on arc length) refines only three or four orbit parameters. The second step of our gravity estimation method accommodates orbit error in the components corresponding to P_8, P_{10}, and P_{11} (and also P_1 in long arcs). The tests in Sect. 5 demonstrated that (at least in a relative sense) it is not as important to consider errors arising from the other eight or nine state parameters. Our two-step method requires that the first step produces an input trajectory which is accurate enough that the second step can ignore these eight or nine parameters altogether. As seen in Sect. 6, the input trajectory used in our study was sufficiently accurate. To conclude that discussion, we here demonstrate that the high accuracy of the input trajectory used in this study does not cause overly optimistic results.

The partial derivatives of the intersatellite measurement with respect to state parameters were examined for a sample of arcs. This examination was restricted to the nine unrefined parameters. Of these nine, four can be excluded based on the size of the maximum partial derivative found. According to the partial derivatives, any one of these four parameters could contain an error corresponding to 10 cm and the resulting range-rate signal would never reach 1 μm s^{-1} for any observation over a 15-minute arc. These parameters are P_2, P_3 (the declination and right ascension of the baseline midpoint), P_9, and P_{12} (the baseline yaw parameters), and it is intuitive that the range-rate observation would be insensitive to them. Parameters P_4, P_5, and P_6 (corresponding to the velocity vector of the system midpoint) can be taken as a group. When the measurement partials of these parameters are taken as a triple to form a vector at any epoch of the arc, they are linearly dependent with the initial velocity vector of the arc. This implies that an error in any one component is unimportant, and that only an error in the magnitude of the system midpoint velocity vector is possibly important. It takes an error of about 25 μm s^{-1} in the initial velocity vector of the system midpoint to affect any range-rate observation over a 15-minute arc at the 1 μm s^{-1} level. According to Kepler's third law, for a satellite at an altitude of 500 km, an error of 25 μm s^{-1} in the initial velocity vector is equivalent to about 5 cm radial error. Radial errors of 5 cm should be attainable. Furthermore, as shown below, the adjusting elements (P_8, P_{10}, P_{11}) can accommodate radial error.

There are only two parameters, P_1 (the system midpoint height) and P_7 (baseline length), that cannot be excluded from causing problems by the examination of measurement partial derivatives. Extra orbit tests were performed for these two parameters. The input trajectory was altered systematically in these components. The first 41 short arcs were re-run with altered input

trajectories. Four additional sets of runs were made for these 41 arcs. The first two sets of runs were made with the 'truth' (EGM96) gravity field. In the first set of runs, the input trajectory was altered so that the midpoint height value was 5 cm smaller than on the original input trajectory. In the second set of runs, the trajectory which had already been altered radially was further altered to make the baseline longer by 10 cm. The fits in these runs were unaltered by the use of the modified trajectories. The maximum residual was 0.12 μm s^{-1}. It should be noted that the alterations of the input trajectory did cause a slight change in the values of the adjusted parameters, especially P_{10} (baseline velocity magnitude). The same two modified input trajectories were used for the final two sets of runs. These two sets of runs use the clone gravity field and, as in the corresponding set of runs which use the original input trajectory, the residuals in these runs (7–25 μm s^{-1} RMS) are the result of gravity errors. The residual pattern is what determines the adjustment of the gravity coefficients, and our objective was to determine if the use of the modified input trajectories affected the residual pattern. Each of the 6929 observation residuals in these final two sets was differenced with the corresponding residual in the original set of runs (the set using the original input trajectory). The maximum residual difference was 0.11 μm s^{-1}.

References

Bertiger WI, Bar-Sever YE, Christensen EJ, Davis ES, Guinn JR, Haines BJ, Jee JR, Lichten SM, Melbourne WG, Muellerschoen RJ, Munson TN, Vigue Y, Wu SC, Yunck TP, Schuntz BE, Abusali PAM, Rim HJ, Watkins MM, Willis P (1994) GPS precise tracking of Topex/Poseidon: results and implications. J Geophys Res 99: 24 449–24 464

Colombo OL (1984) The global mapping of gravity with two satellites. Netherlands Geodetic Commission, Delft

Colombo OL (1989) The dynamics of Global Positioning System orbits and the determination of precise ephemerides. J Geophys Res 94: 9167–9182

Douglas BC, Goad CC, Morrison FF (1980) Determination of the geopotential from satellite-to-satellite tracking data. J Geophys Res 85: 5471–5480

Jekeli C (1999) The determination of gravitational potential differences from satellite-to-satellite tracking. Celest Mech Dynam Astro 75: 85–101

Jekeli C, Rapp RH (1980) Accuracy of the determination of mean anomalies and mean geoid undulations from a satellite gravity field mapping mission. Rep 307, Department of Geodetic Science, The Ohio State University, Columbus

Jekeli C, Upadhyay TN (1990) Gravity estimation from STAGE, a satellite-to-satellite tracking mission. J Geophys Res 95: 10 973–10 985

Kahn WD, Klosko SM, Wells WT (1982) Mean gravity anomalies from a combination of Apollo/ATS-6 and GEOS-3/ATS-6 SST tracking campaigns. J Geophys Res 87: 2904–2918

Kaula WM (1983) Inference of variations in the gravity field from satellite-to-satellite range rate. J Geophys Res 88: 8345–8349

Lemoine FG, Kenyon SC, Factor JR, Trimmer RG, Pavlis NK, Chinn DS, Cox CM, Klosko SM, Luthcke SB, Torrence MH, Wang YM, Williamson RG, Pavlis EC, Rapp RH, Olson TR (1998a) The development of the joint NASA GSFC and NIMA geopotential model EGM96. NASA Tech memo 206861, Goddard Space Flight Center, Greenbelt, MD

Lemoine FG, Cox CM, Chinn DS, Torrence MH, Pavlis NK, Wang YM, Pavlis EC (1998b) Gravitational models including TDRSS data from EP/EUVE, RXTE, ERBS, CGRO, and TRMM (abstract). EOS Trans Am Geophys Un 79: S56

Lerch FJ (1991) Optimum data weighting and error calibration for estimation of gravitational parameters. Bull Géod 65: 44–52

National Research Council (1997) Satellite gravity and the geosphere. National Academy Press, Washington, DC

Pavlis DE, Poulose S, Rowton SC, McCarthy JJ (2001) GEODYN II system documentation, Raytheon ITSS Contractor rep, Greenbelt, MD

Reigber C, Luehr H, Schwintzer P (2000) CHAMP mission status and perspectives (abstract). EOS, Trans Am Geophys Un 81: F307

Rowlands DD, Luthcke SB, Marshall JA, Cox CM, Williamson RG, Rowton SC (1997) Space shuttle precision orbit determination in support of SLA-1 using TDRSS and GPS tracking data J. Astronaut Sci 45: 113–129

Schwintzer P, Reigber C, Barthelmes F, Bode A, Gruber T, Koenig R, Biancale R, Balmino G, Lemoine J-M, Loyer S, Perosanz F (2000) Gravity field recovery from CHAMP: first results (abstract). EOS, Trans Am Geophys Un 81: F307

Sinclair AT, Appleby GM (1993) A short-arc method for determination of station coordinates and baselines applied in the Mediterranean area. In: Smith DE, Turcotte D (eds) Contributions of space geodesy to geodynamics. American Geophysical Union, Washington, pp 389–396

Tapley BD, Reigber C (2000) The GRACE mission: status and future plans (abstract). EOS, Trans Am Geophys Un 81: F307

Verhagen AA, Schrama EJO, Bouman J (2000) Time variations in the gravity field due to atmospheric pressure variations (abstract). EOS, Trans Am Geophys Un 81: F311

Vonbur FO (1972) The ATS/Nimbus tracking experiment. In: Melchoir P, Yumi S (eds) Rotation of the Earth. Reidel, Dordrecht, pp 112–120

Wagner CA (1983) Direct determination of gravitational harmonics from low-low Gravsat data. J Geophys Res 88: 309–321

Wagner CA (1987) Improved gravitational recovery from a geopotential research mission satellite pair flying en echelon. J. Geophys Res 92: 8147–8155

Wolff M (1969) Direct measurements of the earth's gravity potential using a satellite pair. J Geophys Res 74: 5292–5300

Zlotnicki V, Fukumori I, Hirose N, Menemenlis D, Ali A (2000) Dealiasing GRACE: the high-frequency ocean response to wind and pressure (abstract). EOS, Trans Am Geophys Un 81: F308